

The influence of metallic particle size on the mechanical properties of polytetrafluoroethylene-Al–W powder composites

J. Cai and V. F. Nesterenko^{a)}

Materials Science and Engineering Program, University of California at San Diego, La Jolla, California 92093-0418, USA

K. S. Vecchio and F. Jiang

Department of NanoEngineering, University of California at San Diego, La Jolla, California 92093-0418, USA

E. B. Herbold and D. J. Benson

Department of Mechanical and Aerospace Engineering, University of California at San Diego, La Jolla, California 92093-0411, USA

J. W. Addiss, S. M. Walley, and W. G. Proud

Cavendish Laboratory, Madingley Road, Cambridge CB3 0HE, United Kingdom

(Received 25 September 2007; accepted 18 December 2007; published online 24 January 2008)

The dynamic mechanical properties of high density mixtures of polytetrafluoroethylene, aluminum (Al), and tungsten (W) powders are tailored by changing the morphology of the particles and porosity. Powder composites with fine metallic particles exhibited higher ultimate compressive strength, despite higher porosity, than less porous composites containing coarse W particles with equivalent mass fractions. The mesoscale force chains between the fine metallic particles are responsible for this unusual phenomenon. Macrocracks forming in the sample below the critical failure strain in the matrix and a competition between densification and fracture were observed in dynamic tests. © 2008 American Institute of Physics. [DOI: 10.1063/1.2832672]

Polytetrafluoroethylene (PTFE) and aluminum (Al) mixtures are known to be energetic under dynamic and/or thermal loading.^{1–7} This paper considers the mechanical behavior of PTFE-Al-W composites where tungsten (W), with varying particle size, was used to increase density. A Eulerian hydrocode is used to model the composite behavior.

Varying particle size and morphology in pressed⁸ or polymer bonded^{9,10} explosives or layer thicknesses in laminates¹¹ significantly alter the mechanical properties, shock sensitivity, and the rate of energy release. The mesoscale force-chain formation in granular energetic materials can be related to ignition sites under compressive load.^{12–14}

Cold isostatic pressing (CIPing) was used to prepare specimens from a mixture of 17.5 wt % PTFE, 5.5 wt % Al, and 77 wt % W powders. The powder granules had an approximately spherical shape with the following diameters: Al: 2 μm , coarse W powder: $<44 \mu\text{m}$ and fine W powder with particle size $<1 \mu\text{m}$ and PTFE: 100 nm. The mixtures of powders were ball milled in the SPEX 800 mill for 2–10 min using alumina balls to reduce agglomeration.

Table I lists the density and volume fraction of pores of specimens. Note that under the same CIPing conditions, the density of PTFE-Al–W with fine W particles was 6 g/cm³ while the density of PTFE-Al–W with coarse W particles was 7.1 g/cm³, which is close to the theoretical density. At the same pressing condition, the mixture of PTFE and Al powders can be fully densified.¹⁵ Specimens containing coarse W particles were also processed at a significantly reduced CIPing pressure (20 MPa). This resulted in a porosity similar to those with fine W particles.

A typical solid cylindrical specimen is 10 mm high and 10.44 mm in diameter. Three to six samples of each type of

composite were tested under the same conditions. Dynamic testing was performed using a Hopkinson bar with transmitting bar made from magnesium alloy. A “soft” drop-weight test was developed to allow effective testing of low strength specimens at higher strains.¹⁶ The results of these tests are presented in Table I.

The results in Table I demonstrate an unusual phenomenon when comparing samples with fine W particles and higher porosity to those with coarse W particles and a lower porosity. Curiously, the samples with higher porosity exhibited a higher ultimate compression strength in experiments; usually higher porosity leads to lower material strength. Comparing the strengths of the porous PTFE-Al-fine W and the porous PTFE-Al-coarse W, it is clear that porosity itself does not contribute to the higher strength of the porous composite filled with fine W particles.

The porous samples with coarse W particles demonstrated an unusual behavior.¹⁶ Some samples exhibited a very low strength and failed in shear at ~ 11 MPa in drop weight tests. Other samples failed at a considerably greater stress of 40 MPa. The higher compressive strength may be attributed to the gradual densification during the initial deformation resulting in a considerably increased strength relative to samples that fail almost immediately. This phenomenon can be expected when the ultimate compressive strength is higher than the densification pressure (in this case, 20 MPa) used to prepare samples. This was not observed for porous samples with fine metallic particles or denser samples with coarse W particles. There is clearly some competition occurring between the compaction of the soft viscoelastic matrix and macrofracture during the deformation process.

A porous sample, with coarse W particles where the deformation was interrupted at an engineering strain of 0.1, has failed by shear localization.¹⁶ Separation of metal particles from the matrix and the fracture of matrix were two major

^{a)}Electronic mail: vnesterenko@ucsd.edu.

TABLE I. Properties of various specimens and their quasistatic and dynamic strength.

		Dense PTFE-Al-coarse W	Porous PTFE-Al-fine W	Porous PTFE-Al-coarse W	Pure dense PTFE
Size of W particles (μm)		<44	<1	<44	...
CIPing pressure (MPa)		350	350	20	350
Density (g/cm^3)		7.1 ± 0.4	6.0 ± 0.3	6.0 ± 0.3	2.1 ± 0.1
Porosity (%)		1.6	14.3	14.3	4.5
Ultimate compressive strength (MPa)	Quasistatic tests (10^{-3} s^{-1})	18 ± 1	22 ± 6	5.8 ± 0.2	2.3 ± 0.3
	Hopkinson bar tests (500 s^{-1})	30 ± 1	45 ± 7	10 ± 3	21 ± 3
	Drop-weight tests (300 s^{-1})	32 ± 2	55 ± 6	$11 \pm 2(40 \pm 11)$...

mesoscale mechanisms for failure.¹⁷ The mesoscale mechanism of shear localization at low levels of strain is considered in (Ref. 18) and examples of shear localization due to microfracture mechanisms leading to reaction in granular materials can be found in (Ref. 19 and 20).

Two-dimensional granular packings were used for modeling of shock compaction²¹ and photoelastic disks as analogs of energetic materials in the literature,^{13,14} though the two-dimensional metallic particle mesostructure of the composites do not reproduce the coordination number as in three-dimensional packings. Two samples using random mixture of fine ($1 \mu\text{m}$) W and Al particles ($2 \mu\text{m}$) (sample 1)²⁶ and coarse ($10 \mu\text{m}$) W and Al particles ($2 \mu\text{m}$) (sample 2) of circular shape are used in finite element calculations. The weight and volume fractions of each sample constituent were similar in the calculations (e.g., volume fractions: 59% PTFE, 28% W, and 13% Al) and experiments.²²

A two-dimensional Eulerian Hydrocode is implemented to simulate the behavior of the samples at high strain rates in drop weight tests. Each material in the sample had separate equations of state, physical, and mechanical properties without interfacial strength. The failure strength for PTFE (0.05) was determined from Hopkinson bar tests of pure CIPed PTFE samples. The Johnson-Cook²³ material model was used for all materials and the constants were determined from previous literature data.²⁴ The Gruneisen form of the equation of state was used to define the pressure in compression and tension for PTFE.²⁵ The equation of state used for

W and Al was linear elasticity since the particle deformation during dynamic loading is minimal. The numerical values of all parameters are listed elsewhere.²⁶

The numerical analysis shows that the first compressive stress maxima of sample 1 (Fig. 1, curve 1) is 85 MPa and the corresponding stress of sample 2 at 35 MPa (Fig. 1, curve 2) is significantly lower. The von Mises stress distribution for the sample with fine tungsten particles is shown in Figs. 2 and 3. Figure 2 shows the stress distribution within the sample at 0.022 “global” strain. A single force chain is apparent starting from the top left center through the bottom of the sample. This can be compared to the sudden increase in the stress-strain plot shown in curve 1 in Fig. 3 at the corresponding strain. Upon further deformation, this force chain disintegrates and a macrocrack starts in the matrix at a global strain less than the critical failure strain of matrix material (0.05), resulting in the decrease in stress in curve 1 (Fig. 1). Thus, the maximum global stress attained in experiments may occur after the onset of failure in the matrix.

Force chains propagating through the cracks in the matrix are reactivated upon further deformation (see the stress distribution corresponding to the global strain 0.238, Fig. 3). This self organization of force chains was accompanied by a macrocrack formed diagonally from the top right to the bottom left (Fig. 3), which is in qualitative agreement with the observed failure in experiments.¹⁶ The corresponding local effective plastic strain in the sample (see Fig. 6 in Ref. 27) above this crack shows that the damage in the PTFE matrix is distributed around the metal particles.

Additional features can be observed relating to the first sample where fine W and Al particles facilitated the presence of force chains. The vertical and horizontal displacements of the metallic particles, initiated by the vertical displacement of the top boundary, are comparable to their sizes resulting in force chains being created, destroyed, and reactivated with

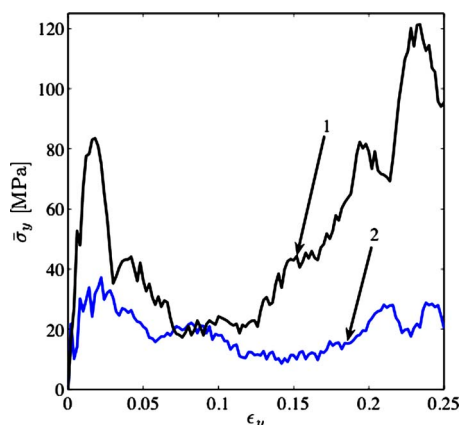


FIG. 1. (Color online) Average engineering stress at the top of the sample plotted against the global strain for a sample with small W particles (sample 1, curve 1) and a sample using large W particles (sample 2, curve 2). Note the stress increases in curve 1 after 0.13 global strain while the curve 2 coincides with the results for pure CIPed PTFE (not shown).

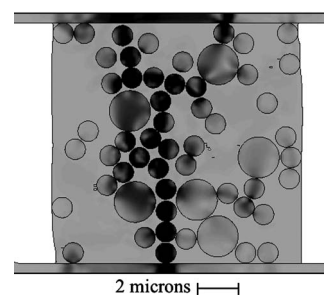


FIG. 2. True stress distribution at 0.022 global strain for sample 1. The color intensity varies from light gray (0 MPa) to dark gray (≥ 50 MPa).

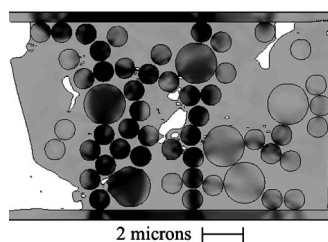


FIG. 3. True stress distribution at 0.238 global strain for sample 1. The color intensity varies from light gray (0 MPa) to dark gray (≥ 50 MPa).

different particles. It is interesting that the progressive local fracture of PTFE matrix corresponds to the spikes of global stress (curve 1, Fig. 1) and the global stress in the highest peak is observed in the heavily fractured sample (Fig. 3). This is because the disintegration of matrix is accompanied by local dense packing of metal particles resisting further deformation. After the initiation of the macrocrack, part of the sample was left undeformed. This type of behavior should be avoided since the initiation of a reaction between components will not occur in such areas.

The second sample did not have a particle distribution conducive to force chain activation. “Through-thickness” force chains are not present in this sample up to 0.25 global strain, though localized short chains and the macrocracks were formed. Separate calculations (not shown) with a pure PTFE sample have a stress strain behavior very similar to curve 2 in Fig. 1. This suggests that mainly the matrix material in sample 2 resisted the load. The vertical and horizontal displacements of the metal particles in the second sample are also comparable to their sizes and to the size of the sample. The metal particles also initiated shear macrocracks in the PTFE matrix propagating at 45° from the direction of compression similar to those observed in the experiments.¹⁶

The presented calculations demonstrated that force chains created by circular metallic particles in the investigated materials are a probable cause of the higher strength of these mixtures. This is a different mechanism than the one proposed for higher strength of composites with smaller particles, which was related to the difference in paths of crack propagation in matrix for polymer bonded explosives.⁹

This is also supported by comparing the volume fraction of metallic particles in CIPed mixtures with PTFE and the volume fraction of them (taken at the same mass ratio as in the mixture) at tapped densities.²⁰ The combined volume fraction of fine W and fine Al particles in the mixture with PTFE for a CIPed sample with density of 6 g/cm^3 is 0.36. This is higher than the volume fraction of the granules (0.27) in the tapped mixture of fine W and fine Al taken at the same mass ratio as in the mixture with PTFE. This means that the force chains supporting the mesostructure in this tapped powder will also be present in the CIPed composite sample.

This is not the case with a composite sample using coarse W and fine Al (density of 7.1 g/cm^3) which was CIPed at the same pressure as the sample with fine W particles. Here, the volume fraction of metal particles is significantly smaller (0.425) than the volume fraction of the granules (0.69) in the tapped mixture of coarse W and fine Al powders taken at the same mass ratio as in the mixture with PTFE. This means that PTFE matrix is dispersing metal particles preventing them from forming force chains.

Based on this comparison, it is reasonable to assume that given the same constituent mass fractions, the strength of a composite will be higher when the volume fraction of the metallic particles is comparable to the corresponding value in tapped metallic powders. This volume fraction can be significantly smaller than in a dense random packing of spherical particles (0.64) and it should depend on the shape of granules. Also, the dependence of the ultimate sample strength on particle size should be sensitive to particle shape.

It was demonstrated that the dynamic mechanical properties of high density mixtures of PTFE, aluminum, and tungsten powders can be tailored by changing the size of the particles and porosity of the mixture. The mesoscale force chains between the fine metallic particles significantly contribute to the strength of the composites with small W particles. The macrocracks below the critical failure strain for the matrix and a competition between densification and fracture in dynamic tests were observed.

The support for this project provided by ONR (N00014-06-1-0263 and MURI ONR Award N00014-07-1-0740) and the EPSRC (J. W. Addiss) is highly appreciated.

- ¹J. J. Davis, A. J. Lindfors, P. J. Miller, S. Finnegan, and D. L. Woody, 11th International Detonation Symposium, 1998 (unpublished), p. 1007.
- ²W. H. Holt, W. Mock, Jr., and F. Santiago, *J. Appl. Phys.* **88**, 5485 (2000).
- ³N. M. McGregor and G. T. Sutherland, *AIP Conf. Proc.* **706**, 1001 (2004).
- ⁴A. Y. Dolgoborodov, M. N. Makhov, I. V. Kolbanev, A. N. Streletskii, and V. E. Fortov, *JETP Lett.* **81**, 311 (2005).
- ⁵R. Ames, *Multi-function Energetic Materials*, MRS Symposia Proceedings No. 896 (Materials Research Society, Pittsburgh, 2006), p. 123.
- ⁶A. A. Denisaev, A. S. Steinberg, and A. A. Berlin, *Dokl. Phys. Chem.* **414**, 139 (2007).
- ⁷S. M. Walley, J. E. Balzer, W. G. Proud, and J. E. Field, *Proc. R. Soc. London, Ser. A* **456**, 1483 (2000).
- ⁸R. E. Setchell, *Combust. Flame* **56**, 343 (1984).
- ⁹C. R. Siviour, M. J. Gifford, S. M. Walley, W. G. Proud, and J. E. Field, *J. Mater. Sci.* **39**, 1255 (2004).
- ¹⁰J. E. Balzer, C. R. Siviour, S. M. Walley, W. G. Proud, and J. E. Field, *Proc. R. Soc. London, Ser. A* **460**, 781 (2004).
- ¹¹A. B. Mann, A. J. Gavens, M. E. Reiss, D. Van Heerden, G. Bao, and T. P. Weihs, *J. Appl. Phys.* **82**, 1178 (1997).
- ¹²J. C. Foster, Jr., J. G. Glenn, and M. Gunger, *AIP Conf. Proc.* **505**, 703 (2000).
- ¹³S. G. Bardenhagen and J. U. Brackbill, *J. Appl. Phys.* **83**, 5732 (1998).
- ¹⁴K. M. Roessig, J. C. Foster, Jr., and S. G. Bardenhagen, *Exp. Mech.* **42**, 329 (2002).
- ¹⁵J. Cai and V. F. Nesterenko, *AIP Conf. Proc.* **845**, 793 (2006).
- ¹⁶J. Addiss, J. Cai, S. M. Walley, W. G. Proud, and V. F. Nesterenko, *AIP Conf. Proc.* **955**, 773 (2007).
- ¹⁷J. Cai, S. M. Walley, R. J. A. Hunt, W. G. Proud, V. F. Nesterenko, and M. A. Meyers, *Mater. Sci. Eng., A* **472**, 308 (2008).
- ¹⁸T. N. Dey and J. N. Johnson, *AIP Conf. Proc.* **429**, 285 (1998).
- ¹⁹C. J. Shih, V. F. Nesterenko, and M. A. Meyers, *J. Appl. Phys.* **83**, 4660 (1998).
- ²⁰V. F. Nesterenko, *Dynamics of Heterogeneous Materials* (Springer, New York, 2001), Chap. 2.
- ²¹D. J. Benson, V. F. Nesterenko, F. Jonsdottir, and M. A. Meyers, *J. Mech. Phys. Solids* **45**, 1955 (1997).
- ²²J. Cai, F. Jiang, K. S. Vecchio, M. A. Meyers, and V. F. Nesterenko, *AIP Conf. Proc.* **955**, 773 (2007).
- ²³G. R. Johnson and W. H. Cook, in *Proceedings of the Seventh International Symposium on Ballistics*, The Hague, Netherlands, 1983 (unpublished), Vol. 541, p. 1.
- ²⁴F. J. Zerilli and R. J. Armstrong, *AIP Conf. Proc.* **620**, 657 (2002).
- ²⁵D. J. Steinberg, “Equation of state and strength properties of selected materials,” Report No. UCRL-MA-106439, 1996.
- ²⁶E. B. Herbold, J. Cai, D. J. Benson, and V. F. Nesterenko, *AIP Conf. Proc.* **955**, 785 (2007).
- ²⁷E. B. Herbold, J. Cai, D. J. Benson, and V. F. Nesterenko, e-print arXiv:0708.1205v1.